REPORT No. 867

A THEORETICAL INVESTIGATION OF HYDRODYNAMIC IMPACT LOADS ON SCALLOPED-BOTTOM SEAPLANES AND COMPARISONS WITH EXPERIMENT

By Benjamin Milwitzky

SUMMARY

An analytical method is presented for calculating the hydrodynamic impact loads and motions experienced by seaplane floats and hulls with scalloped (fluted) bottoms. The analysis treats vertical impact at zero trim in addition to the more general problem of the step impact of a seaplane at positive trim where the flight path is oblique to the keel and to the water surface. Also considered are the transformations required to represent impacts into waves.

The analysis, which is equally applicable to floats having cross sections of any shape, considers that the flow about an immersing planing bottom occurs largely in transverse flow planes which are normal to the keel. The equations of motion are written in general terms and require the determination of the virtual water mass as a function of the depth of penetration of the keel into the flow planes. On the basis of a simple extension of Wagner's expanding-plate analogy, equations are presented whereby the section characteristics, which determine the virtual mass, may be calculated for any given float shape.

In order to illustrate the applicability of the analysis to practical problems, time histories of the applied hydrodynamic load have been calculated for specific impact conditions and are compared with Langley impact-basin test data obtained in smooth and rough water with a double-scalloped-bottom seaplane float which is representative of current commercial and service types.

INTRODUCTION

Investigations conducted by the National Advisory Committee for Aeronautics during the past several years have indicated that current seaplane design specifications are inadequate and that more rational means are required for predicting hydrodynamic loads. In order to provide further information on the problem of impact loads, an analytical and experimental research program is now in progress at the Langley impact basin, the theoretical phase of which has resulted in the investigations presented in references 1 and 2, which deal primarily with V-bottom floats.

The present paper extends the general investigation to include an analytical method for calculating the loads on scalloped-(fluted) bottom floats, which is also applicable to floats and hulls of other shapes. Interest in this problem

was occasioned by failures in the course of service operations of seaplane floats which had successfully withstood static tests in excess of design requirements.

The analysis derives the equations governing the vertical impact of a float at zero trim in addition to those for the more general problem of the step impact of a seaplane at positive trim along a flight path inclined to the water surface. The approximations necessary to represent impacts into waves are also considered. The equations of motion are written in general terms and require the determination of the section characteristics, which define the variation of virtual mass with penetration, for the float under consideration. Based on a simple modification of Wagner's expanding-plate analogy, equations are presented from which the section characteristics may be calculated for any given float shape.

In order to illustrate the degree of applicability of the method, the results of calculations for several specific impact conditions are presented in the form of hydrodynamic load-time histories and are compared with corresponding impact-basin test data obtained in smooth and rough water with the float shown in figures 1 and 2. This float, which has a double scalloped bottom and conventional lines, is representative of current commercial and service types.
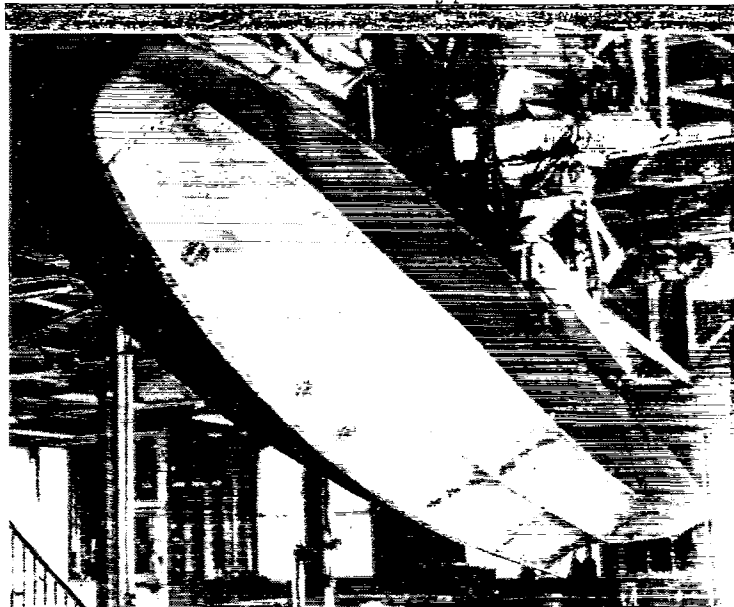

Figure 1.—View of scalloped-bottom seaplane float tested in the Langley impact basin.
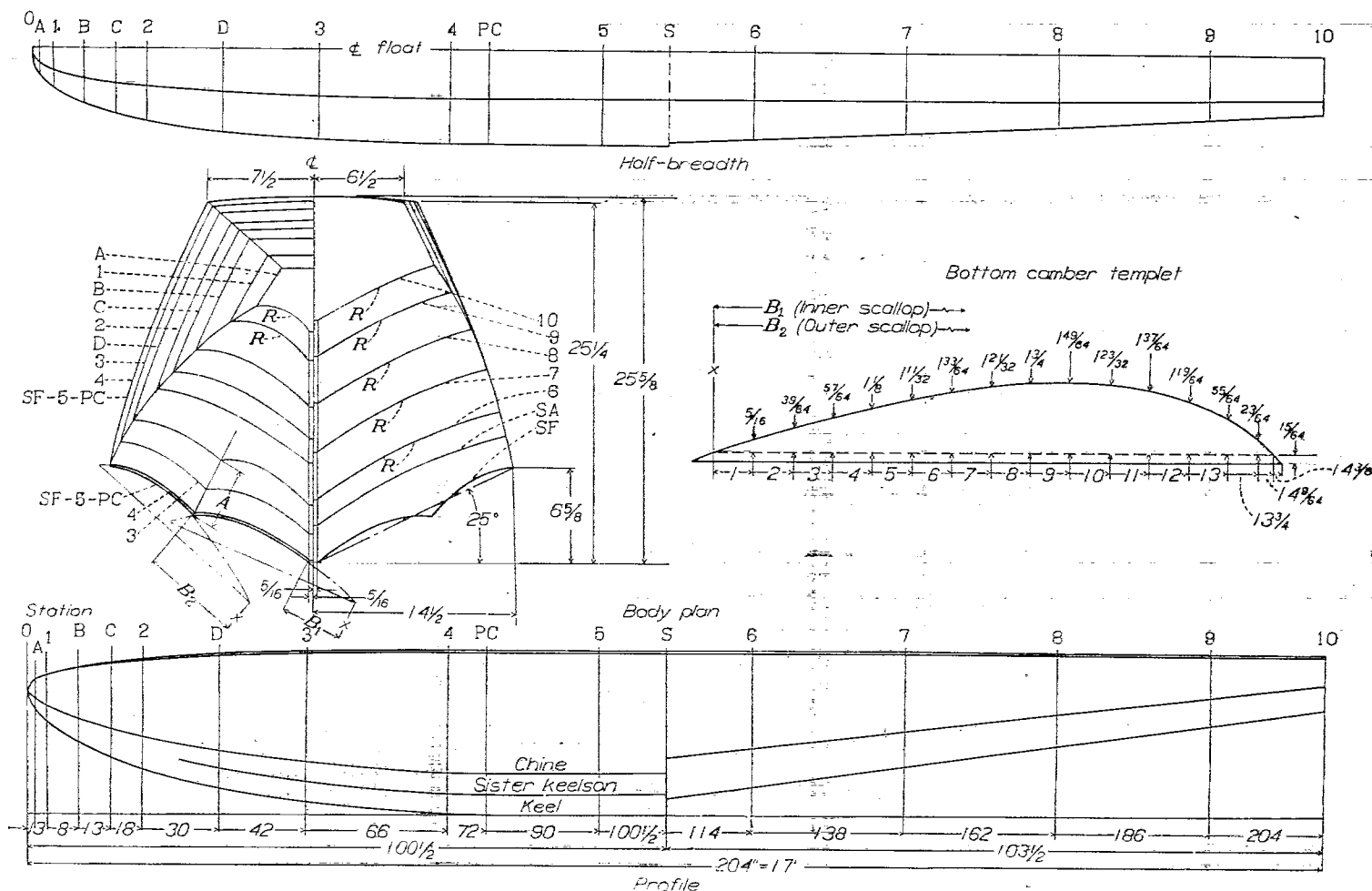
FIGURE 2.—Lines of scalloped-bottom seaplane float tested in Langley impact basin.

SYMBOLS

A_{ij} coefficients in shape matrix for inner scallop

B_{ij} coefficients in shape matrix for outer scallop

a_j coefficients in series expansion of u for inner scallop

b_j coefficients in series expansion of u for outer scallop

A aspect ratio of immersed part of float

c wetted semiwidth at any station along keel

F resultant force

g acceleration due to gravity

l length of forebody

M total mass of seaplane $\left(\dfrac{W}{g}\right)$

m_w virtual mass at any station

n_{i_v} impact load factor $\left(-\dfrac{\ddot{z}}{g}\right)$

s longitudinal distance from a given flow plane to foremost immersed point along keel

t time after contact

u expansion ratio $\left(\dfrac{d\zeta/dt}{dc/dt}\right)$

V velocity of float

v local fluid velocity

V_w translational velocity of wave

W total weight of seaplane

ξ distance parallel to keel

η transverse distance from axis of symmetry

ζ penetration of any cross section measured normal to keel from undisturbed water surface

x horizontal distance

y transverse distance from axis of symmetry (coincident with η)

z draft at step measured normal to water surface

β angle of dead rise

γ flight-path angle

θ angle of wave slope with horizontal

ρ mass density of water

τ trim angle

Subscripts:

0   initial conditions

ch at instant of chine immersion

e effective

h horizontal

n normal to keel

p parallel to keel

r resultant
s for cross section at step
sk at instant of "sister keelson" immersion
v vertical
$calc$ calculated
mod modified

ANALYSIS

When a long narrow shape such as a keeled seaplane float or flying-boat hull penetrates the surface of a large stationary body of water, the primary flow of the neighboring fluid tends to occur in transverse planes (reference 1) which are essentially perpendicular to the length of the body, as contrasted with the largely longitudinal flow in the case of high-aspect-ratio wings. In the present analysis the flow planes in the water are considered fixed in space and oriented normal to the axis of the body, the effects of end losses and longitudinal components of flow being included as an aspect-ratio correction. This approach simplifies the problem, especially when the keel line of the float is not parallel to the surface, since it permits the flow in any given plane to be considered a purely two-dimensional phenomenon independent of all other flow planes.

The flow process within a particular flow plane begins when the keel of the float passes through the water surface and penetrates the plane. At all times thereafter, the momentum imparted to the water in the plane is determined solely by the increase in the float cross-sectional shape intersected by the plane and may be expressed as the product of the virtual mass m_w associated with the immersed cross section and the velocity of penetration into the plane. In potential flow the virtual mass is determined by the intersected float shape and may thus be considered a function of the penetration ζ into the flow plane.

When a seaplane contacts the water surface, the resultant velocity is oblique to the keel. Thus, in addition to the velocity of penetration into the flow planes (normal to the keel), a longitudinal velocity component of considerable magnitude will also usually exist. In a perfect fluid, if the float is of constant cross section, motion normal to a flow plane will not affect the growth of the intersected cross section and its virtual mass. For any penetration the momentum of the fluid in a given plane thus depends only on the velocity of penetration and is unaffected by motion of the float parallel to its axis. This condition exists, however, only so long as the plane under consideration remains in contact with the float. After the step has passed through a particular flow plane, the intersected cross section ceases to exist and the plane becomes part of the downwash where it remains, thereafter, independent of the subsequent progress of the impact. As a result, the force acting on the float is governed by the growth of the immersed shape and the motion normal to the keel, while the total momentum lost by the float is distributed between the water directly beneath the keel and the downwash behind the step.

On the basis of the foregoing application of the virtual-mass concept, the following sections of the analysis treat the vertical immersion at zero trim of a float of constant cross section, in addition to the more general problem of impact at positive trim along a flight path inclined to the water surface. In both cases the weight of the seaplane is assumed to be balanced by the wing lift. Also considered are the approximate transformations required to represent impacts into waves. The equations of motion presented have general applicability to any float shape regardless of how the virtual mass may be determined. A subsequent section of the analysis deals specifically with methods for calculating the virtual mass for cross sections of arbitrary shape.

IMPACT NORMAL TO THE WATER AT ZERO TRIM

The simplest impact problem is that of the vertical immersion of a prismatic float when the keel is parallel to the water surface. If m_w is the virtual mass in any flow plane, the total virtual mass is $m_w l$, except for end losses. From tests conducted with vibrating plates, Pabst (reference 3) determined an end-loss correction to the virtual mass. This factor may be written $1 - \dfrac{1}{2A}$, where A is the aspect ratio. In the present problem, since the resultant velocity is normal to the keel, the same flow planes are in contact with the float throughout the impact process and the initial momentum of the float is at all times distributed between the float and the water directly beneath. Therefore,

$$\dot{\zeta} = \frac{M\dot{\zeta}_0}{M + \left(1 - \dfrac{1}{2A}\right)m_w l} = \frac{\dot{\zeta}_0}{1 + \left(1 - \dfrac{1}{2A}\right)\dfrac{m_w l}{M}} \quad (1)$$

and

$$-\ddot{\zeta} = \frac{\dot{\zeta}\dot{\zeta}_0\left[\left(1 - \dfrac{1}{2A}\right)\dfrac{dm_w}{d\zeta} + \dfrac{m_w}{2A^2}\dfrac{dA}{d\zeta}\right]}{\dfrac{M}{l}\left[1 + \left(1 - \dfrac{1}{2A}\right)\dfrac{m_w l}{M}\right]^2} \quad (2)$$

The determination of m_w and A as functions of the penetration, as well as the solution of the equations of motion, will be discussed in a subsequent section.

OBLIQUE IMPACT AT POSITIVE TRIM

In an oblique impact along a flight path inclined to the keel, because of the component of velocity parallel to the keel, the same flow planes are not always in contact with the float. As a result of the consequent loss of momentum to the downwash, the initial momentum of the float cannot be considered distributed solely between the float and the water directly beneath the keel, as was assumed in arriving at equations (1) and (2) which therefore apply only when the resultant velocity is normal to the keel.

Figure 3 is a schematic representation of the oblique impact of a scalloped-bottom float at positive trim. The motion of the float may be referred to the coordinates ξ, η, and ζ, which are parallel and normal to the keel, or to the coordinates x, y, and z, which are parallel and normal to the water surface. The point where the step first contacts the water surface is taken as the origin of the latter coordinate system. In figure 3, ζ is the depth of penetration of the keel (measured normal to the keel from the undisturbed water surface) into a given flow plane which is fixed in space. While ζ may be considered attached to the flow plane, the dimension ζ_s, on the other hand, is a measure of the penetration of the step and moves with the float. The draft at the step z is a projection of ζ_s normal to the water surface. In an oblique impact, therefore,

$$\dot{\zeta}_s = \dot{\zeta} - V_p \tan \tau \qquad (3)$$

In any flow plane the virtual mass is m_w. In the flow plane at the step, the virtual mass is designated m_{w_s}.

On a two-dimensional basis, the momentum imparted to the fluid in any flow plane is $m_w \dot{\zeta}\,ds$. Differentiation of the momentum determines the force contributed by a given plane

$$dF = (m_w \ddot{\zeta} + \dot{\zeta}\,\dot{m}_w)\,ds \qquad (4)$$

For a keeled float at positive trim, if the small effect of the scallops on the aspect ratio is neglected, A is constant during the impact and equal to $\tan \beta/\tan \tau$, where β is the average dead-rise angle (fig. 3), so that the aspect-ratio correction factor is $1 - \dfrac{\tan \tau}{2 \tan \beta}$. Integrating along the length gives the total force on the float normal to the keel:

$$F = \left(1 - \frac{\tan \tau}{2 \tan \beta}\right)\left(\ddot{\zeta}\int_0^{\frac{\zeta_s}{\tan \tau}} m_w\,ds + \dot{\zeta}\int_0^{\frac{\zeta_s}{\tan \tau}} \dot{m}_w\,ds\right)$$

Since $\dfrac{\zeta}{s} = \tan \tau$,

$$F = K\left(\ddot{\zeta}\int_0^{\zeta_s} m_w\,d\zeta + \dot{\zeta}^2 \int_0^{m_{w_s}} dm_w\right) \qquad (5)$$

where

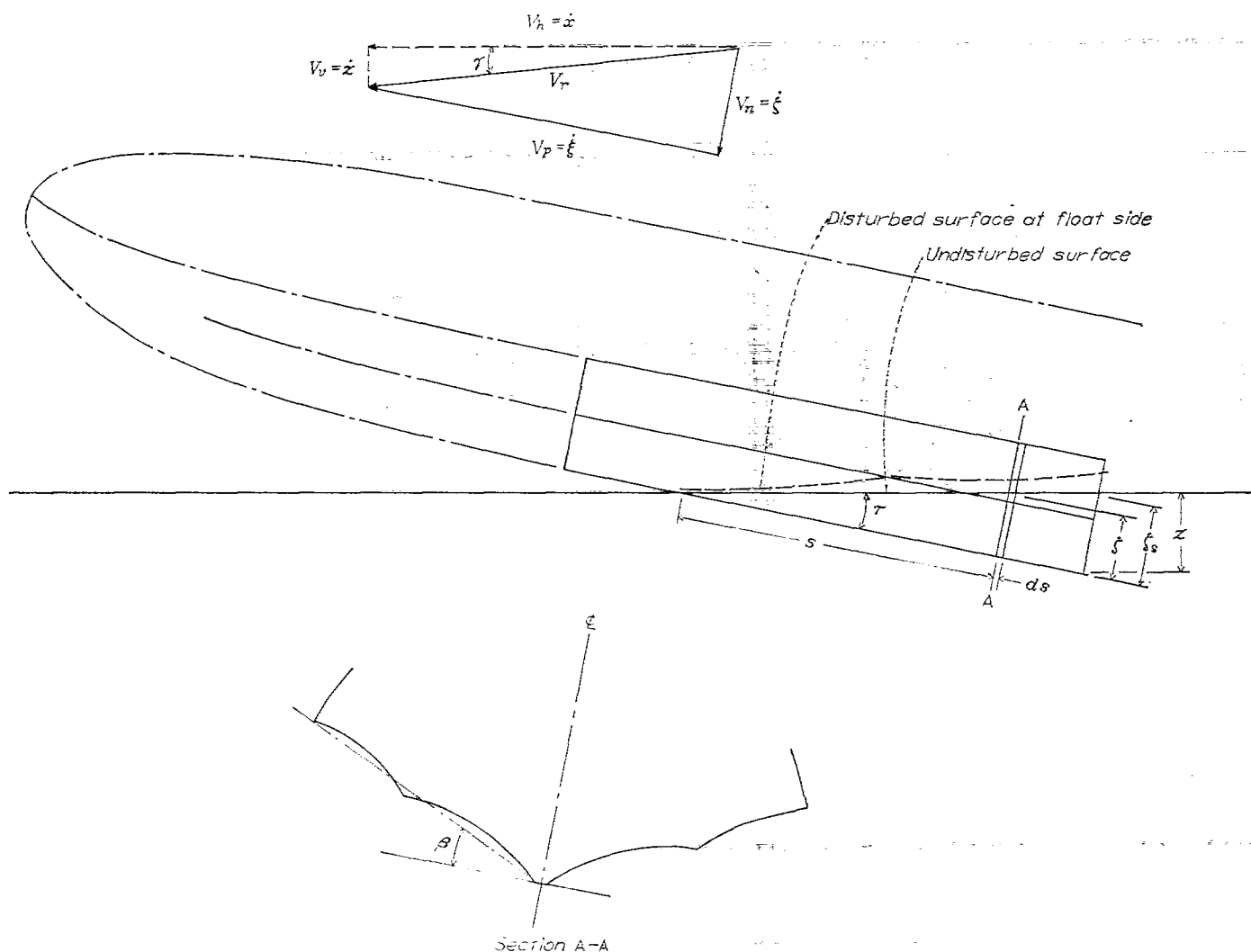$$K = \frac{1}{\tan \tau}\left(1 - \frac{\tan \tau}{2 \tan \beta}\right)$$

FIGURE 3.—Immersion of scalloped-bottom float.

During the impact the trim angle and the wing lift are assumed essentially constant, the latter being equal to the weight of the seaplane W. Therefore, application of Newton's second law yields

$$-\frac{W}{g}\ddot{\zeta}=K\left[\ddot{\zeta}\int_0^{\zeta_s}m_w d\zeta+\dot{\zeta}^2 m_{w_s}\right] \tag{6}$$

For a float of constant cross section,

$$\int_0^{\zeta_s}m_w d\zeta=\int_0^{\zeta_s}m_{w_s}d\zeta_s$$

Thus, the equation of motion may be written

$$-\ddot{\zeta}=\frac{\dot{\zeta}^2 m_{w_s}}{\dfrac{W}{Kg}+\displaystyle\int_0^{\zeta_s}m_{w_s}d\zeta_s} \tag{7}$$

Since, for a prismatic float immersing a frictionless fluid, the reaction in each flow plane is normal to the keel, the total force is normal to the keel. As a result, there is no longitudinal acceleration and the velocity component parallel to the keel $\dot{\xi}$ is at all times constant and equal to its initial magnitude V_p. Thus, differentiating equation (3) gives

$$\ddot{\zeta}=\ddot{\zeta}_s \tag{8}$$

Applying equations (3) and (8) permits equation (7) to be rewritten as follows:

$$-\int_0^{\zeta_s}\frac{\ddot{\zeta}_s d\zeta_s}{(\zeta_s+V_p\tan\tau)^2}=\int_0^{\zeta_s}\frac{m_{w_s}d\zeta_s}{\dfrac{W}{Kg}+\displaystyle\int_0^{\zeta_s}m_{w_s}d\zeta_s} \tag{9}$$

Integrating equation (9) and substituting the relationship between $\dot{\zeta}$ and $\dot{\zeta}_s$ gives

$$V_p\tan\tau\left(\frac{1}{V_{n_0}}-\frac{1}{\dot{\zeta}}\right)-\log_e\frac{\dot{\zeta}}{V_{n_0}}=\log_e\left(1+\frac{Kg}{W}\int_0^{\zeta_s}m_{w_s}d\zeta_s\right)$$

and

$$\frac{W}{Kg}\left(\frac{V_{n_0}}{\dot{\zeta}}e^\lambda-1\right)=\int_0^{\zeta_s}m_{w_s}d\zeta_s \tag{10}$$

where

$$\lambda=V_p\tan\tau\left(\frac{1}{V_{n_0}}-\frac{1}{\dot{\zeta}}\right)$$

For convenience in comparing the theoretical results with experimental data obtained in laboratory testing, the foregoing equations may be rewritten in terms of the coordinates relative to the water surface. From figure 3 it can be readily seen that

$$\dot{\zeta}=\dot{x}\sin\tau+\dot{z}\cos\tau \tag{11}$$

and

$$\dot{\xi}=\dot{x}\cos\tau-\dot{z}\sin\tau$$

$$=V_p=V_{h_0}\cos\tau-V_{s_0}\sin\tau \tag{12}$$

Combining equations (11) and (12) gives

$$\dot{\zeta}=\frac{\dot{z}}{\cos\tau}+K_1 \tag{13}$$

where

$$K_1=V_p\tan\tau$$

$$=(V_{h_0}-V_{s_0}\tan\tau)\sin\tau$$

Differentiating equation (13) gives

$$\ddot{\zeta}=\ddot{\zeta}_s=\frac{\ddot{z}}{\cos\tau} \tag{14}$$

Substituting equations (13) and (14) in equation (7) yields

$$-\ddot{z}=\frac{(\dot{z}+K_1\cos\tau)^2 m_{w_s}}{\cos\tau\left(\dfrac{W}{Kg}+\displaystyle\int_0^{\zeta_s}m_{w_s}d\zeta_s\right)} \tag{15}$$

and equation (10) may be written

$$\frac{W}{Kg}\left[\left(\frac{V_{s_0}+K_1\cos\tau}{\dot{z}+K_1\cos\tau}\right)e^\mu-1\right]=\int_0^{\zeta_s}m_{w_s}d\zeta_s \tag{16}$$

where

$$\mu=K_1\cos\tau\left(\frac{1}{V_{s_0}+K_1\cos\tau}-\frac{1}{\dot{z}+K_1\cos\tau}\right)$$

Under certain contact conditions the penetration of the float may become sufficiently great to require the determination of the effect of chine immersion on the later stages of the time history. The foregoing equations are valid throughout the impact process and are equally applicable after the chines have become submerged.

As the float penetrates a particular flow plane the virtual mass increases until the chines reach the water surface, after which the virtual mass may be assumed to remain constant and equal to its magnitude at the time of chine immersion. Thus, after chine immersion has occurred the preceding equations may be applied with the following substitutions:

$$m_{w_s}=m_{w_{s_{ch}}}$$

and

$$\int_0^{\zeta_s}m_{w_s}d\zeta_s=\int_0^{\zeta_{s_{ch}}}m_{w_s}d\zeta_s+m_{w_{s_{ch}}}(\zeta_s-\zeta_{s_{ch}}) \tag{17}$$

Appendix A contains working equations for the two types of impacts treated in the preceding analysis in a form directly suitable for computation. The determination of the virtual mass is based on a method presented in a subsequent section of the report, which is applicable to float cross sections of any shape.

IMPACT IN ROUGH WATER

As a first approach toward the calculation of hydrodynamic loads in seaway, the preceding analysis may be applied to rough-water impacts if the initial conditions are defined relative to the wave surface. For trochoidal waves with large length-amplitude ratio, the wave profile may be simulated by

an inclined plane tangent to the surface at the point of contact, which serves as the effective frame of reference for the foregoing equations.

The preceding assumptions fail to consider the internal orbital velocities and displacements of the fluid particles within the wave and are therefore approximate. At best, the procedure should be applied only to impacts where the float contacts the wave about half way between trough and crest for those cases where the trim is equal to or greater than the slope of the wave.

The initial effective horizontal velocity (parallel to wave slope) is given by

$$V_{h_{e_0}} = (V_{h_0} + V_w) \cos \theta - V_{v_0} \sin \theta \qquad (18)$$

and the initial effective vertical velocity (normal to wave slope) is

$$V_{v_{e_0}} = (V_{h_0} + V_w) \sin \theta + V_{v_0} \cos \theta \qquad (19)$$

where V_w is the translational velocity of the wave and θ is the angle of the wave slope with the horizontal. The effective trim relative to the wave is

$$\tau_e = \tau - \theta \qquad (20)$$

With the effective initial conditions $V_{h_{e_0}}$, $V_{v_{e_0}}$, and τ_e replacing the smooth-water conditions V_h, V_{v_0}, and τ, the foregoing equations of motion may be considered to apply to impacts into waves within the restrictions noted.

For comparison with experimental data representing the actual vertical motion of the seaplane, the effective magnitudes of the vertical displacement z_e, vertical velocity $\dot{z}_e$, and vertical acceleration $\ddot{z}_e$ calculated by application of the foregoing equations may be converted to the corresponding components relative to the true vertical axis by the relationships

$$z = V_{v_0}t + \left(z_e - V_{v_{e_0}}t\right)(1 - \tan \tau_e \tan \theta) \cos \theta \qquad (21)$$

$$\dot{z} = V_{v_0} + \left(\dot{z}_e - V_{v_{e_0}}\right)(1 - \tan \tau_e \tan \theta) \cos \theta \qquad (22)$$

and

$$\ddot{z} = \ddot{z}_e(1 - \tan \tau_e \tan \theta) \cos \theta \qquad (23)$$

DETERMINATION OF THE VIRTUAL MASS

The preceding equations of motion have been written in general terms and are applicable to any float shape; however, before practical impact solutions can be obtained for a specific float, the virtual mass of the cross-sectional shape under investigation must be determined as a function of the penetration. Because of a number of mathematical obstacles, a rigorous determination of the flow about such immersing shapes is quite difficult and general solutions have not been obtained.

In the specific case of the V-bottom, where the immersed cross-sectional shapes in a given flow plane are always similar

and the flow patterns at different degrees of penetration may be considered models of each other, the virtual mass can be determined from the results of an iterative solution made by Wagner (reference 4) to calculate the force on a V-shape of 18° dead rise immersing with constant velocity. The results for the particular case of 18° were extended to other dead-rise angles by the equation

$$F = \left(\frac{\pi}{2\beta} - 1\right)^2 \rho \pi \zeta \dot{\zeta}^2$$

The virtual mass corresponding to this equation may be evaluated quite simply by recognizing that, for constant-velocity penetration, the force is due solely to the increase in virtual mass accompanying the enlarging flow pattern and, according to equation (4), is given by $\dot{\zeta} \dot{m}_w$. By equating Wagner's force equation with the quantity $\dot{\zeta} \dot{m}_w$ and integrating, the corresponding virtual mass for the V-shape is found to be

$$m_w = \left(\frac{\pi}{2\beta} - 1\right)^2 \frac{\rho \pi}{2} \zeta^2$$

In reference 1 a comparison of this value with planing data for V-bottom floats having different dead-rise angles indicated that an empirical factor of 0.82 should be applied to the virtual mass. The introduction of this factor gives a modified value for the virtual mass

$$m_w = 0.82 \left(\frac{\pi}{2\beta} - 1\right)^2 \frac{\rho \pi}{2} \zeta^2 \qquad (24)$$

Applying equation (24) therefore permits the force on a two-dimensional V-shape immersing with variable velocity to be determined as

$$F = 0.82 \left(\frac{\pi}{2\beta} - 1\right)^2 \frac{\rho \pi}{2} (\zeta^2 \ddot{\zeta} + 2\zeta \dot{\zeta}^2) \qquad (25)$$

In the case of more complicated cross sections, however, such as those of scalloped bottoms or floats with chine flare, the immersed shape in any flow plane may vary quite irregularly with penetration, thereby precluding the use of equation (24) for the determination of the virtual mass. In view of the present lack of a more exact solution for the flow about immersing curved or scalloped cross sections, the expanding-plate analogy proposed by Wagner in references 4 and 5 may be applied. This approximation assumes that the momentum of the fluid disturbed by an immersing shape is equal to that of the fluid on one side of an expanding plate in submerged motion having the same velocity as the immersing shape.

The substitution of a flat plate of varying width for the actual shape is based on the concept that the primary disturbance of the fluid about an immersing form takes place in the immediate vicinity of the surface and is due largely to the expansion of the wetted width. Thus, the virtual mass

of an immersing cross section may be taken equal to half the value for a plate in submerged motion; namely,

$$m_w = \frac{\rho \pi c^2}{2} \qquad (26)$$

where c is the semiwidth of the effective plate.

On this basis the problem becomes one of determining how the effective width of the plate varies as the actual cross section immerses. This variation may be considered one of the section characteristics of a given float shape.

Calculation of section characteristics.—Early attempts to approximate the virtual mass of V-shapes did not consider that the water rises along the sides of an immersing body above the level of the original surface and simply assumed that the width of the equivalent plate was equal to the width of the actual cross section in the plane of the undisturbed water surface. In impact calculations, neglect of the rise in determining the virtual mass may lead to erroneous results, especially in the case of scalloped bottoms or floats with reflexed chines where, under certain conditions, infinite loads may be predicted on the basis of this assumption.

In order to consider the increase in wetted width arising from the disturbance of the free surface by the penetration, it may be assumed, as in references 4 and 5, that the fluid particles at the surface move vertically upward and, differences in elevation being neglected, that the velocity distribution at the surface corresponds to that in the plane of a flat plate in submerged motion. By integration of the distributed velocities, the equation of the free surface, the rise of the water in the vicinity of the immersing shape, and the resulting wetted width may be determined. Because of the simplifying assumptions involved in this procedure, the calculated variation of wetted width with penetration may be improved by the application of a simple modification subsequently discussed.

On the basis of the foregoing concepts, the equations for determining the section characteristics are derived by considering the increase in wetted width in a given flow plane due to the disturbance of the free surface. Figure 4 is a schematic representation of a scalloped cross section in the process of immersion. The general equations governing the entire immersion process may be derived by considering the situation at some time after the sister keelson has become submerged.

The wetted semiwidth (determined by the intersection of the disturbed free surface and the cross section) is denoted by c. The local normal velocity v, relative to the float, of a particle in the free surface at a distance $\eta \geq c$ from the axis of
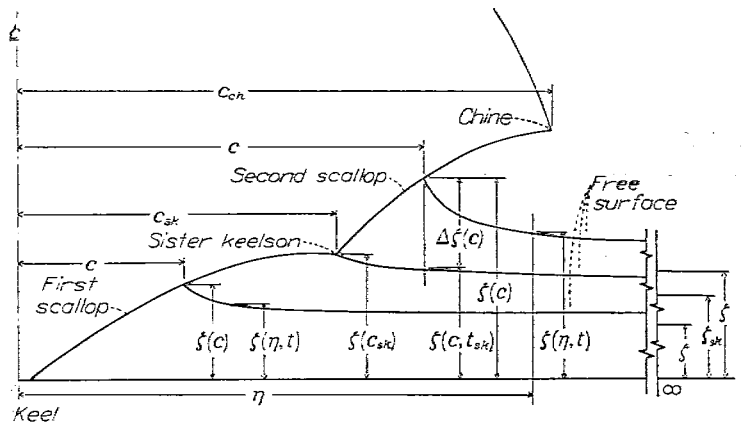

FIGURE 4.—Symbols and definitions for analysis of immersion of scalloped cross section.

symmetry is given in terms of the velocity of penetration $\dot{\zeta}$ by the equation for the velocity distribution in the plane of a flat plate:

$$v = \frac{\dot{\zeta}}{\sqrt{1 - \frac{c^2}{\eta^2}}} \qquad (27)$$

At any instant after initial contact, the vertical displacement of the particle from the keel is $\zeta(\eta, t)$. (See fig. 4.) At the instant of immersion of the sister keelson the displacement is $\zeta(\eta, t_{sk})$. At any later time, therefore, the rise of the free surface from the keel is given by

$$\zeta(\eta, t) = \zeta(\eta, t_{sk}) + \int_{t_{sk}}^{t} \frac{\dot{\zeta} dt}{\sqrt{1 - \frac{c^2}{\eta^2}}} \qquad (28)$$

Equation (28) may be evaluated by considering c the independent variable; thus

$$\zeta(\eta, t) = \zeta(\eta, t_{sk}) + \int_{c_{sk}}^{c} \frac{\dfrac{\dot{\zeta}}{dc/dt} dc}{\sqrt{1 - \frac{c^2}{\eta^2}}} \qquad (28a)$$

and expanding the ratio $\dfrac{\dot{\zeta}}{dc/dt} = \dfrac{d\zeta}{dc} = u(c)$ as a power series gives

$$u(c) = b_1 + b_2 c + b_3 c^2 + b_4 c^3 + b_5 c^4 + \ldots \qquad (29)$$

The expansion is carried to five terms in order to provide sufficient accuracy for typical float cross sections.

Substituting equation (29) into equation (28a) and integrating results in the equation of the free surface with reference to the keel:

$$\zeta(\eta, t) = \zeta(\eta, t_{sk}) + \left\{ b_1 \eta \sin^{-1} \frac{c}{\eta} - b_2 \eta \sqrt{\eta^2 - c^2} + \right.$$

$$b_3 \eta \left(\frac{\eta^2}{2} \sin^{-1} \frac{c}{\eta} - \frac{c}{2} \sqrt{\eta^2 - c^2} \right) + b_4 \eta \left[\frac{(\eta^2 - c^2)^{3/2}}{3} - \eta^2 \sqrt{\eta^2 - c^2} \right] -$$

$$\left. \frac{b_5 \eta}{4} \left[c \sqrt{\eta^2 - c^2} \left(c^2 + \frac{3\eta^2}{2} \right) - \frac{3\eta^4}{2} \sin^{-1} \frac{c}{\eta} \right] + \ldots \right\} \Bigg|_{c_{sk}}^{c} \qquad (30)$$

At the float contour $c=\eta$; therefore, evaluating equation (30) between the limits and substituting gives the displacement from the keel of the intersection of the free surface and the cross section:

$$\zeta(c)=\zeta(c,t_{sk})+b_1c\left(\frac{\pi}{2}-\sin^{-1}\frac{c_{sk}}{c}\right)+b_2c\sqrt{c^2-c_{sk}^2}+$$

$$b_3c\left[\frac{c^2}{2}\left(\frac{\pi}{2}-\sin^{-1}\frac{c_{sk}}{c}\right)+\frac{c_{sk}}{2}\sqrt{c^2-c_{sk}^2}\right]+$$

$$b_4c\left[c^2\sqrt{c^2-c_{sk}^2}-\frac{(c^2-c_{sk}^2)^{3/2}}{3}\right]+\cdots$$

$$\frac{b_5c}{4}\left[c_{sk}\sqrt{c^2-c_{sk}^2}\left(c_{sk}^2+\frac{3c^2}{2}\right)+\frac{3c^4}{2}\left(\frac{\pi}{2}-\sin^{-1}\frac{c_{sk}}{c}\right)\right]+\cdots$$

(31)

The coefficients b_1, b_2, . . . may be evaluated by the solution of the system of equations formed by the substitution in equation (31) of the coordinates c_1, $\zeta(c_1)$; c_2, $\zeta(c_2)$; . . . of several points chosen on the contour of the scallop. This system of equations may be conveniently written in the matrix notation

$$\begin{bmatrix} B_{11} & B_{12} & B_{13} & \ldots & B_{1n} \\ B_{21} & B_{22} & B_{23} & \ldots & B_{2n} \\ B_{31} & B_{32} & B_{33} & \ldots & B_{3n} \\ \cdots & \cdots & \cdots & \cdots & \cdots \\ B_{m1} & B_{m2} & B_{m3} & \ldots & B_{mn} \end{bmatrix} \begin{bmatrix} b_1 \\ b_2 \\ b_3 \\ \cdots \\ b_n \end{bmatrix} = \begin{Bmatrix} [\Delta\zeta(c)]_1 \\ [\Delta\zeta(c)]_2 \\ [\Delta\zeta(c)]_3 \\ \cdots \\ [\Delta\zeta(c)]_m \end{Bmatrix}$$

(32)

where

$$B_{i1}=c_i\left(\frac{\pi}{2}-\sin^{-1}\frac{c_{sk}}{c_i}\right)$$

$$B_{i2}=c_i\sqrt{c_i^2-c_{sk}^2}$$

$$B_{i3}=c_i\left[\frac{c_i^2}{2}\left(\frac{\pi}{2}-\sin^{-1}\frac{c_{sk}}{c_i}\right)+\frac{c_{sk}}{2}\sqrt{c_i^2-c_{sk}^2}\right]$$

$$B_{i4}=c_i\left[c_i^2\sqrt{c_i^2-c_{sk}^2}-\frac{(c_i^2-c_{sk}^2)^{3/2}}{3}\right]$$

$$B_{i5}=\frac{c_i}{4}\left[c_{sk}\sqrt{c_i^2-c_{sk}^2}\left(c_{sk}^2+\frac{3c_i^2}{2}\right)+\frac{3c_i^4}{2}\left(\frac{\pi}{2}-\sin^{-1}\frac{c_{sk}}{c_i}\right)\right]$$

and so forth, and

$$[\Delta\zeta(c)]_i=\zeta(c_i)-\zeta(c_i,t_{sk})$$

The coefficients determined by the solution of equation (32) allow the calculation of $u(c)$ by equation (29). From the definition of $u(c)$, the relationship between the penetration of the cross section ζ (distance between keel and undisturbed water level at infinity) and the wetted width is given by

$$\zeta=\zeta_{sk}+\int_{c_{sk}}^{c}u(c)dc=\zeta_{sk}+b_1(c-c_{sk})+\frac{b_2}{2}(c^2-c_{sk}^2)+$$

$$\frac{b_3}{3}(c^3-c_{sk}^3)+\frac{b_4}{4}(c^4-c_{sk}^4)+\frac{b_5}{5}(c^5-c_{sk}^5)+\cdots \quad (33)$$

from which the section characteristics may be computed.

The preceding derivation is general and applies to any given scallop regardless of the shape or the number of discontinuities comprising the cross section. Before the section characteristics can be calculated for the immersion of a given intermediate scallop, however, the free surface existing at the instant of initial penetration of that scallop must be determined by application of the foregoing equations to the preceding scallop.

For example, in the case of a second scallop the quantities $\zeta(c_i, t_{sk})$ and ζ_{sk} must be, respectively, determined for the time of sister keelson immersion from equations (30) and (33) applied to the first scallop. This solution in turn requires the evaluation of the coefficients for the first scallop, a procedure which is very simple since the water surface is initially flat and $\zeta(c_i, t_0)$ equals zero.

For convenience in application, appendix B contains working equations from which the section characteristics may be directly calculated for each scallop of a double-scalloped float. The equations for determining the section characteristics of the first scallop are similarly applicable to float bottoms having chine flare and no discontinuities between keel and chine.

The unmodified curves in figures 5 and 6 represent the section characteristics calculated for the cross section (station SF) at the step of a conventional scalloped-bottom float, the shape of which has been determined from table I and figure 2 and is also shown in figure 5. The section characteristics computed by the foregoing procedure may be improved by the incorporation of a simple modification.
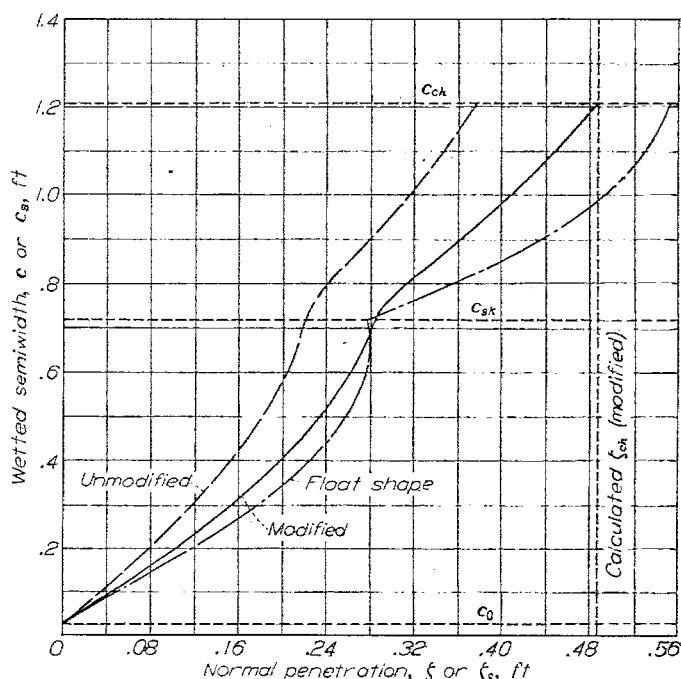

FIGURE 5.—Calculated section characteristics (variation of wetted semiwidth with penetration) for scalloped cross section.

Modification of section characteristics.—Because of the complexity of an exact solution for the flow about an immersing irregular shape such as a scalloped bottom in the vicinity of a free surface, the section characteristics have been approximated by employing Wagner's expanding-plate analogy. In view of the simplifying assumptions involved in this method, the calculated results may be improved by the introduction of a simple modification which results from a comparison of the virtual mass calculated by application of the flat-plate analogy to the case of the V-bottom with the value given by the previously mentioned empirical correction of the results of Wagner's iterative solution for the same case.
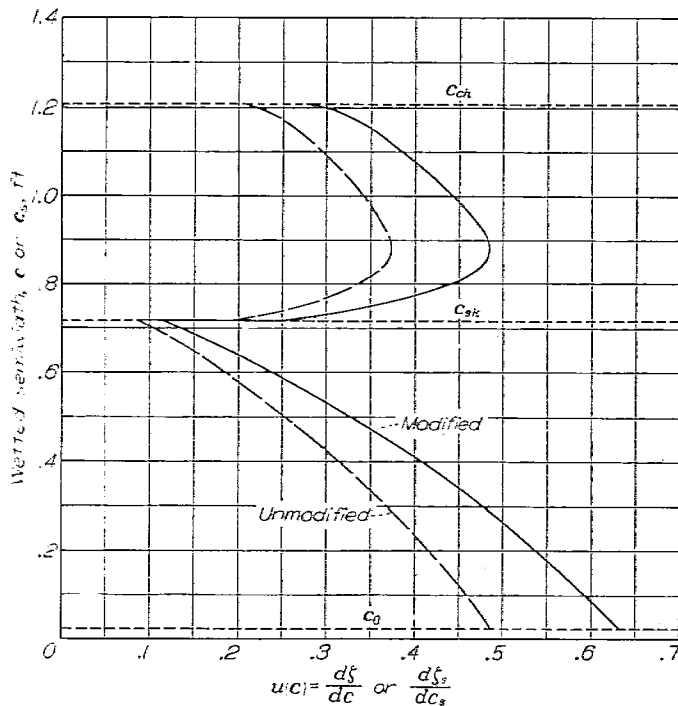
It has been previously pointed out that calculations based on a value of the virtual mass equal to $0.82 \left(\dfrac{\pi}{2\beta}-1\right)^2 \dfrac{\rho\pi}{2}\zeta^2$ have given substantial agreement with tests of a V-bottom float of $22\frac{1}{2}°$ angle of dead rise (reference 1). If this quantity is interpreted to correspond with the virtual mass $\dfrac{\rho\pi c^2}{2}$ on one side of an effective plate of width $2c$, the relationship between the semiwidth of the plate and the penetration of the V-shape is given by

$$c=\sqrt{0.82}\left(\frac{\pi}{2\beta}-1\right)\zeta$$

On the other hand, the application to the V-bottom of the flat-plate analogy employed herein results in a somewhat different variation of width with penetration; namely, $c=\left(\dfrac{\pi}{2}\cot\beta\right)\zeta$. Thus, for a given wetted width the penetration calculated by the flat-plate analogy for a V-shape is $\dfrac{\sqrt{0.82}\left(\dfrac{\pi}{2\beta}-1\right)}{\dfrac{\pi}{2}\cot\beta}$ times that obtained from the empirical correction of the iterative solution.

In the case of an irregular cross section such as that of a scalloped-bottom float, the modification required to correct properly the section characteristics calculated by application of the flat-plate analogy is obviously a variable depending on the shape and penetration. In view of the present lack of a more exact procedure, however, it is suggested that the preceding ratio be applied as a first approximation, at least until further refinements can be effected in the method. The previously calculated curves of ζ and $u(c)$ against c therefore have been modified in accordance with the relation

$$\zeta_{mod}=\frac{\dfrac{\pi}{2}\cot\beta}{\dfrac{\pi}{2\beta}-1}\zeta_{calc} \tag{34}$$

FIGURE 6.—Calculated variation of $u(c)$ with wetted semiwidth for scalloped cross section.

TABLE I

TABLE OF OFFSETS FOR SCALLOPED-BOTTOM FLOAT

[All offsets, in inches, are given to outside of frames and do not include thickness of plating]

Station	Half-breadth			Height above datum line					Bottom details				Station
	Deck	Chine	Sister keelson	Keel	Chine	Sister keelson	Deck side	Deck crown	A ordinate	R	B_1 (inner)	B_2 (outer)	
0	$\frac{5}{16}$	$\frac{5}{16}$	$\frac{5}{16}$	19	19	19	19	19	$17\frac{3}{4}$	------	------	------	0
A	$2\frac{3}{16}$	4	$1\frac{1}{4}$	$16\frac{1}{4}$	$17\frac{21}{32}$	$17\frac{7}{32}$	$20\frac{5}{8}$	$20\frac{21}{32}$	$15\frac{3}{4}$	4	------	------	A
1	$3\frac{3}{16}$	$5\frac{31}{32}$	$2\frac{5}{16}$	$14\frac{5}{8}$	$16\frac{3}{4}$	$15\frac{23}{32}$	$21\frac{1}{4}$	$21\frac{9}{16}$	$14\frac{1}{32}$	$6\frac{3}{4}$	------	------	1
B	$4\frac{15}{32}$	$8\frac{1}{4}$	$3\frac{5}{16}$	$10\frac{31}{32}$	$14\frac{25}{32}$	$13\frac{1}{32}$	$22\frac{5}{8}$	$22\frac{3}{4}$	$11\frac{11}{32}$	------	$4\frac{25}{32}$	------	B
C	$5\frac{1}{4}$	$10\frac{1}{32}$	$4\frac{1}{4}$	$8\frac{25}{32}$	$13\frac{5}{16}$	$11\frac{9}{16}$	$23\frac{9}{32}$	$23\frac{15}{32}$	$9\frac{1}{32}$	------	$2\frac{1}{32}$	------	C
2	$5\frac{13}{16}$	$11\frac{9}{16}$	$5\frac{1}{32}$	$7\frac{7}{16}$	$12\frac{1}{8}$	$10\frac{1}{16}$	$23\frac{25}{32}$	24	$7\frac{21}{32}$	------	$\frac{1}{8}$	------	2
D	$6\frac{11}{16}$	$12\frac{25}{32}$	$6\frac{9}{16}$	$4\frac{1}{32}$	$9\frac{29}{32}$	$7\frac{9}{32}$	$24\frac{17}{32}$	$24\frac{13}{16}$	$4\frac{3}{8}$	------	$2\frac{9}{32}$	$4\frac{3}{32}$	D
3	$7\frac{9}{32}$	$13\frac{27}{32}$	$7\frac{1}{32}$	$2\frac{1}{32}$	$8\frac{1}{32}$	$5\frac{1}{8}$	$24\frac{31}{32}$	$25\frac{1}{16}$	$2\frac{1}{16}$	------	$4\frac{1}{16}$	6	3
4	$7\frac{1}{2}$	$14\frac{15}{32}$	$8\frac{19}{32}$	$\frac{3}{32}$	$6\frac{23}{32}$	$3\frac{3}{8}$	$25\frac{1}{4}$	$25\frac{5}{8}$	$\frac{3}{16}$	------	$4\frac{1}{4}$	$7\frac{1}{4}$	4
PC	$7\frac{1}{2}$	$14\frac{1}{2}$	$8\frac{5}{8}$	0	$6\frac{5}{8}$	$3\frac{3}{16}$	$25\frac{1}{4}$	$25\frac{5}{8}$	0	------	$4\frac{9}{32}$	$7\frac{1}{32}$	PC
5	$7\frac{1}{2}$	$14\frac{1}{2}$	$8\frac{5}{8}$	0	$6\frac{5}{8}$	$3\frac{3}{16}$	$25\frac{1}{4}$	$25\frac{5}{8}$	0	------	$4\frac{9}{32}$	$7\frac{1}{32}$	5
SF	$7\frac{1}{2}$	$14\frac{1}{2}$	$8\frac{5}{8}$	0	$6\frac{5}{8}$	$3\frac{5}{16}$	$25\frac{1}{4}$	$25\frac{5}{8}$	0	------	$4\frac{9}{32}$	$7\frac{1}{32}$	SF
SA	$7\frac{1}{2}$	$13\frac{15}{16}$	------	0	$2\frac{1}{32}$	$8\frac{29}{32}$	$25\frac{1}{4}$	$25\frac{5}{8}$	------	$37\frac{13}{32}$	------	------	SA
6	$7\frac{1}{2}$	$13\frac{15}{32}$	------	$4\frac{13}{32}$	$10\frac{1}{32}$	------	$25\frac{1}{4}$	$25\frac{5}{8}$	------	$35\frac{13}{32}$	------	------	6
7	$7\frac{7}{16}$	$12\frac{1}{2}$	------	$7\frac{3}{4}$	$13\frac{7}{8}$	------	$25\frac{1}{4}$	$25\frac{5}{8}$	------	$31\frac{27}{32}$	------	------	7
8	$7\frac{1}{4}$	$11\frac{11}{32}$	------	$11\frac{1}{16}$	$16\frac{7}{32}$	------	$25\frac{1}{4}$	$25\frac{19}{32}$	------	$28\frac{1}{4}$	------	------	8
9	$6\frac{29}{32}$	$9\frac{15}{16}$	------	$14\frac{3}{8}$	$18\frac{7}{8}$	------	$25\frac{1}{4}$	$25\frac{9}{16}$	------	$24\frac{11}{16}$	------	------	9
10	$6\frac{1}{2}$	$8\frac{11}{16}$	------	$16\frac{7}{8}$	$20\frac{25}{32}$	------	$25\frac{1}{4}$	$25\frac{17}{32}$	------	22	------	------	10

where β is taken as the average dead-rise angle (fig. 3). The factor $\sqrt{0.82}$, which has been omitted from the modification, is included as part of one of the constants in the equations of motion (appendix B). The modified section characteristics for the scalloped-bottom float investigated are presented in figures 5 and 6.

By application of the relationship between the virtual mass and the width of the equivalent plate (equation (26)), the modified section characteristics for a particular float can be used with figure 7 and the equations of motion given in appendix B to calculate time histories of the hydrodynamic loads and motions experienced by the seaplane for as many impact conditions as may be desired.

APPLICABILITY AND LIMITATIONS

In view of the fact that the present analysis considers a float of constant cross section, there may be some question as to the effects of the pulled-up bow and afterbody in applications to conventional floats. Although the longitudinal warping of the float may be taken into account by more complicated equations, it appears that, since conventional floats and hulls are essentially prismatic for a considerable distance forward of the step, the bow will not cause any important deviation of the loads from those calculated on the basis of constant cross section for normal impacts at positive trim (reference 2).

The afterbody, on the other hand, may exert a much more pronounced influence on the motion of the seaplane, particularly in laboratory testing where, as is sometimes the case, the trim of the model may be fixed at very high positive angles. Under such conditions the load is taken almost entirely by the afterbody while the forebody may not become immersed to any appreciable degree until after the maximum acceleration has been attained. At the lower trims associated with step impacts, on the other hand, the depth of
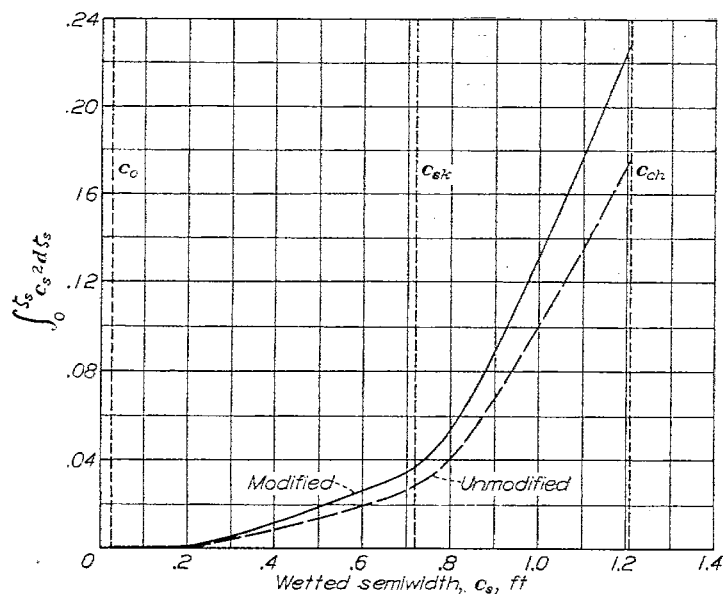
step, the keel angle of the afterbody, and the relatively high longitudinal velocity apparently combine to shield the afterbody so that it carries very little load in comparison with the forebody.

Similarly in flight impacts, even though the landing approach may be made at high trim, the initial contact aft of the step generally results in a downward pitching of the seaplane to the extent that the main impact occurs at reduced trim and corresponds to a forebody impact. The equations presented may thus be considered to represent, approximately, free-flight impacts at high trim if the initial conditions are taken to correspond with those at the beginning of the main impact.

COMPARISON WITH TEST DATA AND DISCUSSION

For the purpose of comparison with experiment, motion time histories have been calculated for several sets of initial conditions corresponding to impact-basin landing tests in smooth and rough water of a full-size scalloped-bottom float. Reference 6 describes the Langley impact basin and its equipment. The all-metal service float used in these tests has underwater lines (see table I and fig. 2) very similar to those of representative service and commercial types. In all cases, the complete float, including afterbody, was tested at fixed trim with a dropping weight of 1350 pounds. Wing lift was simulated by the action of a pneumatic cylinder and cam system, which was designed to apply a constant upward force to the float equal to the dropping weight.

Figures 8 to 15 present comparisons between calculated and measured time histories for various impact conditions. In the figures the accelerations have been converted to impact-load factor n_{i_0} in multiples of the acceleration of gravity.

FIGURE 7.—Calculated variation of $\int_0^{c_{s_*}} c_s{}^2 d\zeta_s$ with wetted semiwidth for scalloped cross section.
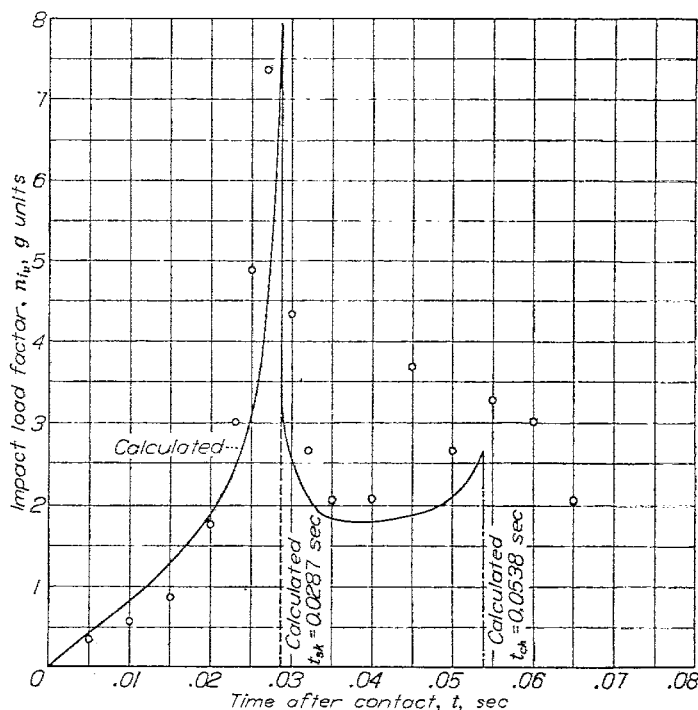

FIGURE 8.—Calculated and experimental time history of hydrodynamic impact load on scalloped-bottom float. Vertical impact; smooth water; $W=1350$ pounds; $V_{v_0}=10.4$ feet per second; $V_{h_0}=0$ feet per second; $\tau=0°$.

In figure 8 the calculated and experimental variations of load with time are shown for an impact normal to the water surface at zero trim. In this case the test data were obtained by means of a dynamometer truss having an estimated natural frequency of the order of 100 cycles per second. The calculations were based on the modified section characteristics presented in figures 5 and 6 and employed an average forebody length of 6 feet to take into account the longitudinal curvature in the bow region.

Since vertical drop at zero trim is the closest practical approximation of a two-dimensional impact and does not involve a loss of momentum to the downwash, the agreement between the theoretical and experimental time histories for this case may be considered a direct indication of the accuracy with which the virtual mass has been determined. In figure 8 the comparison indicates substantial agreement throughout most of the time history and shows the very sharp increase in load as the sister keelson penetrates the surface and a second peak of lesser magnitude at the instant of chine immersion. An unexplained irregularity of the oscillograph record, however, indicated a fluctuation at $t=0.045$ second which is not predicted by the theory.

Figures 9 and 10 present time histories for an oblique impact in smooth water at 3° trim. The experimental data for this condition, as well as for all other oblique impacts presented, were obtained by means of an NACA accelerometer having a natural frequency of 21 cycles per second. Although the comparison in figure 9 shows good agreement during the early stages of the impact, the accelerometer
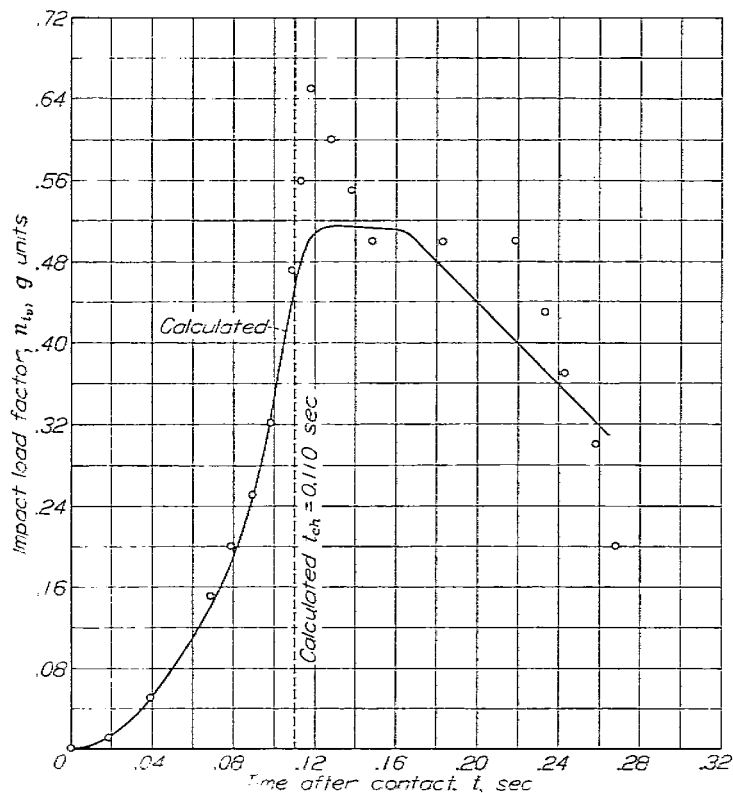
indicated a continuing increase in load beyond the theoretical peak.

Although the response of the accelerometer to the calculated impulse has not been evaluated, at least some of the overshoot is believed due to instrument error or local vibration. A comparison in figure 10 of the displacement and velocity time histories, measured independently by means of a variable resistance slide wire, shows good agreement between the calculated and experimental time histories.

In an attempt to evaluate the accelerometer record further, the measured acceleration time history was integrated mechanically and the velocity variation thus obtained was compared with the calculated velocity time history and that measured by the slide wire. The comparison showed that the three velocity variations agreed very well up to the time when the accelerometer record deviated from the theoretical accelerations but that after this time the velocity curve derived from the accelerometer record indicated a more rapid decrease in velocity than those shown by the theoretical and measured velocity time histories. On the basis of this comparison it appears that the peak accelerometer readings were high and that the actual accelerations were closer to those predicted by the analysis.

In figure 11, a comparison of the acceleration time histories corresponding to an impact in smooth water at 7° trim and medium flight-path angle indicates fairly good agreement between the calculated and measured loads during the impact. The theoretical curve closely follows the accelerometer record and both exhibit the slowly rising load during the initial stages of the impact, the rapid increase just before immersion of the sister keelson, the reduction in the rate of increase of load as the outer scallop becomes immersed, the occurrence of maximum load at the time of chine immersion, and the steady decrease in load accompanying further penetration.
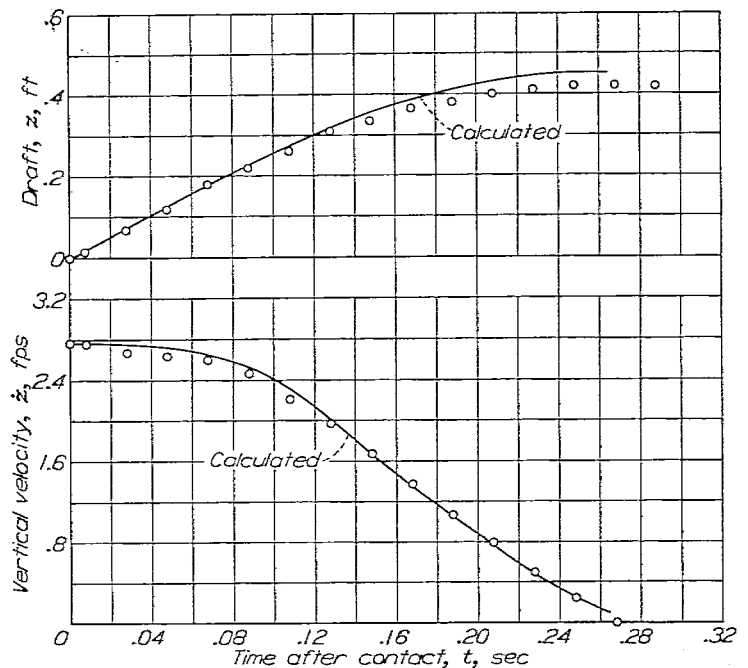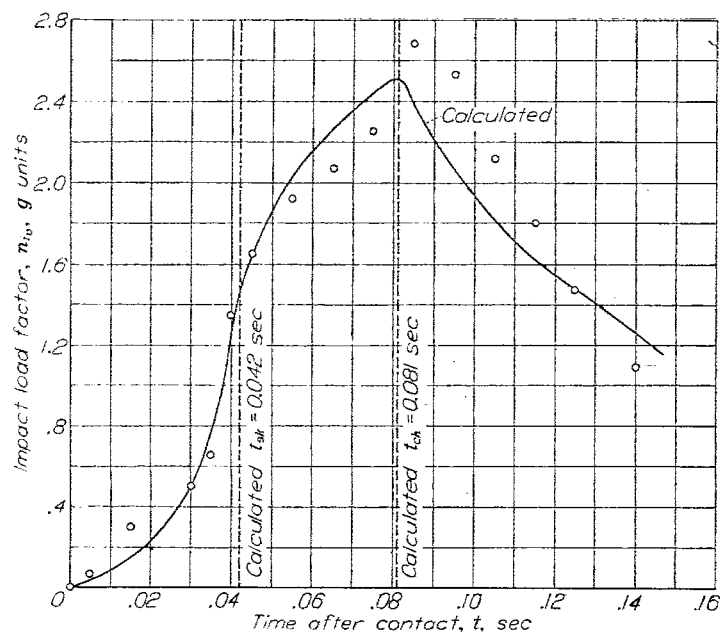

FIGURE 9.—Calculated and experimental time history of hydrodynamic impact load on scalloped-bottom float. Smooth water; $W=1350$ pounds; $V_{x_0}=2.77$ feet per second; $V_{t_0}=55.56$ feet per second; $\tau=3°$.

FIGURE 10.—Calculated and experimental time histories of vertical motion during impact of scalloped-bottom float. Smooth water; $W=1350$ pounds; $V_{x_0}=2.77$ feet per second; $V_{t_0}=55.56$ feet per second; $\tau=3°$.

FIGURE 11.—Calculated and experimental time history of hydrodynamic impact load on scalloped-bottom float. Smooth water; W=1350 pounds; V_{v_0}=6.96 feet per second; V_{h_0}=68.75 feet per second; τ=7°.

A similar comparison is presented in figure 12 for another smooth-water impact at 7° trim but at lower flight-path angle. The agreement is fairly good except in the region of maximum acceleration where the experimental data indicate a sudden drop in load which is not predicted by the theory. Although the behavior of the float denoted by the accelerometer in this region would appear to be unlikely, because of experimental inaccuracies, the source of the discrepancy cannot be definitely determined at the present time.
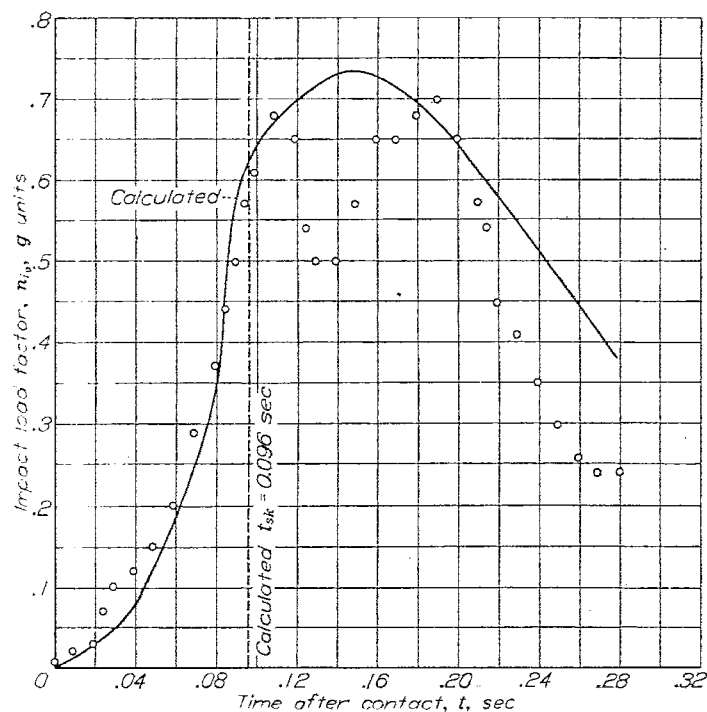
FIGURE 12.—Calculated and experimental time history of hydrodynamic impact load on scalloped-bottom float. Smooth water; W=1350 pounds; V_{v_0}=3.04 feet per second; V_{h_0}=55.2 feet per second; τ=7°.

Time histories which have been calculated for two conditions corresponding to impacts into waves are compared with experiment in figures 13 and 14. In both cases the wave length was 60 feet and the wave height was 2 feet. Figure 13, which presents data corresponding to an impact at 10° trim, shows surprisingly good agreement with experiment, inasmuch as the assumptions involved in the analysis consider the surface of the wave to be simulated by an inclined plane. In figure 14, which represents a rough-water impact at 7° trim, the agreement is not quite as good beyond the time of maximum acceleration.
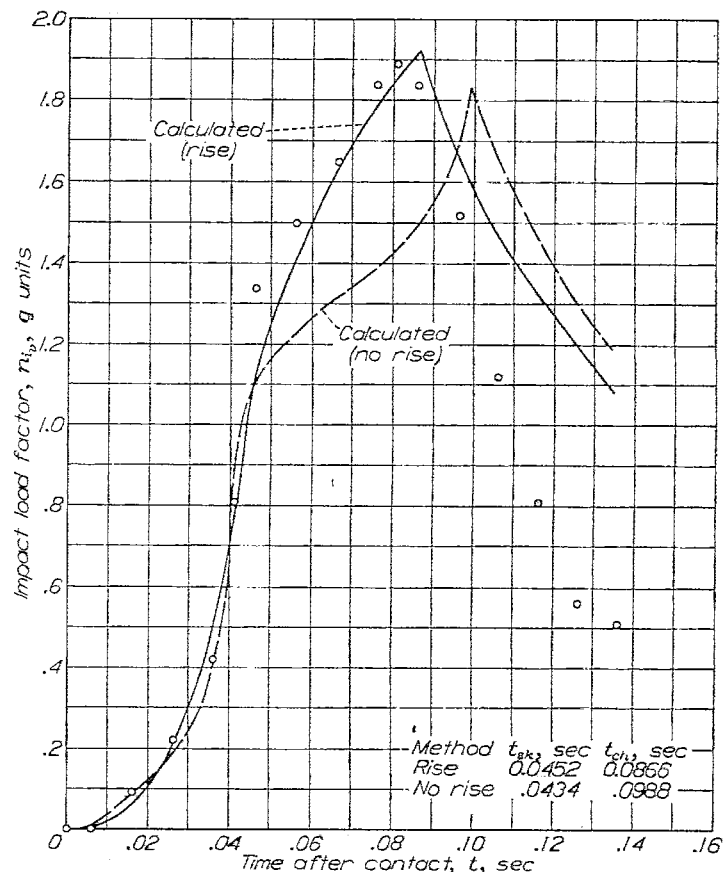
FIGURE 13.—Calculated and experimental time history of hydrodynamic impact load on scalloped-bottom float. Rough water; W=1350 pounds; V_{v_0}=2.77 feet per second; V_{h_0}=49.3 feet per second; τ=10°; wave height, 2 feet; wave length, 60 feet; V_w=12.27 feet per second; θ=3.4°.

In order to illustrate the manner in which seaway may affect the applied loads, the calculated and experimental data of figures 12 and 14 are combined in figure 15. The two time histories shown represent impacts made in smooth and rough water under similar approach conditions and indicate that for the specific conditions presented the maximum load in rough water was somewhat more than three times as great as that encountered in the corresponding smooth-water landing. Furthermore, the time required for the load to reach a maximum after contact was about twice as great in smooth water as in the particular seaway conditions considered.

Since the calculated results are based on a prismatic forebody, the comparisons with experimental data may be

taken to indicate that, for conventional float configurations, the warping of the bow is not important and that the effect of the afterbody is small within the range of trim angles believed to be representative of the main forebody impact in flight landings.

In connection with the behavior of the float during the later stages of the impact, a further examination of the time histories indicates that the measured reduction in load after chine immersion occurred seems to be more rapid than that indicated by the theory. While the analysis incorporated the simplifying assumption that after the chine penetrates
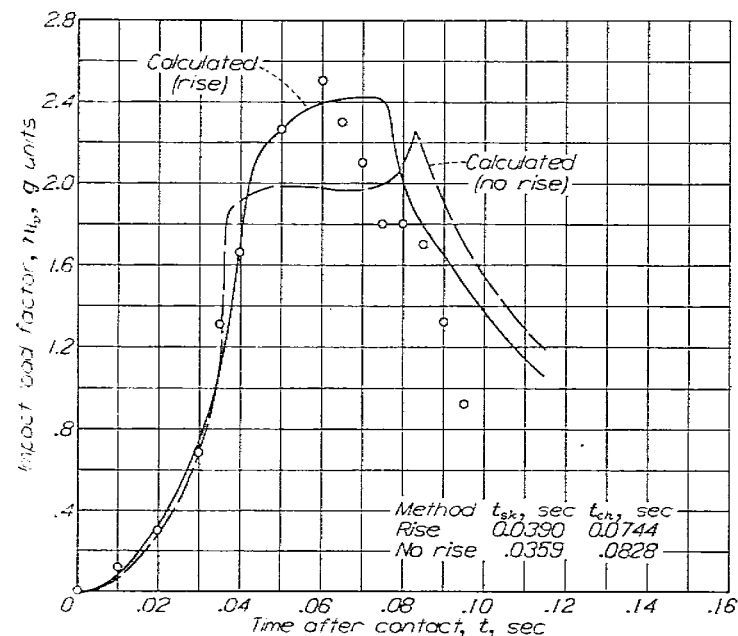

FIGURE 14.—Calculated and experimental time history of hydrodynamic impact load on scalloped-bottom float. Rough water; W=1350 pounds; V'_{v_0}=2.91 feet per second; V'_{h_0}=55.84 feet per second; τ=7°; wave height, 2 feet; wave length, 60 feet; V_w=14.29 feet per second; θ=4°.

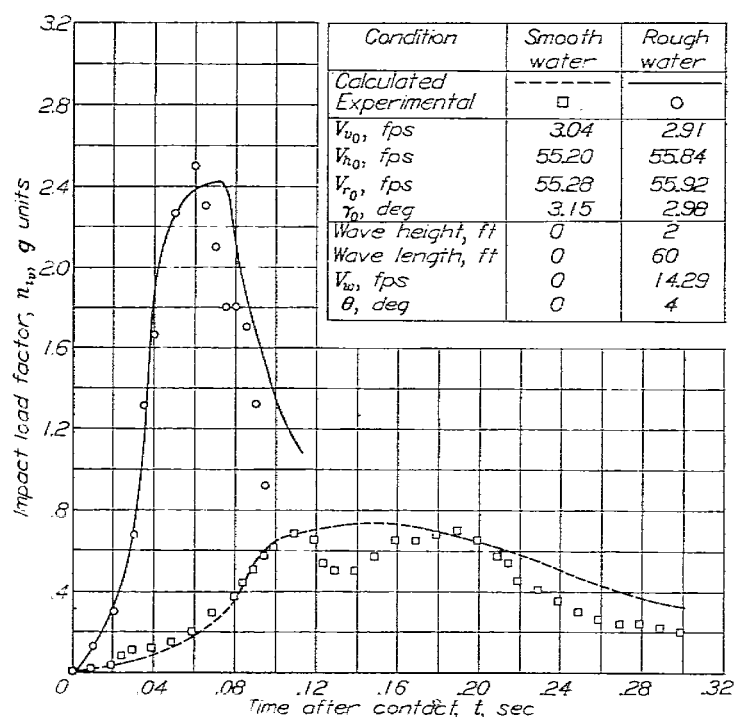FIGURE 15.—Comparison of calculated and experimental time histories of hydrodynamic load on scalloped-bottom float for impacts in smooth and rough water with similar flight conditions. W=1350 pounds; τ=7°

a given flow plane the virtual mass in the plane remains constant and equal to its magnitude at the instant of chine immersion, additional study may lead to a more rigorous method for treating such immersion beyond the chine.

Although it has been pointed out that the local rise of the water should be considered in calculating the virtual mass, use of the geometric shape of the float may suggest itself as an approximation for the calculated section characteristics. Time histories which have been computed on this basis are presented in figures 13 and 14 where they are designated "no rise" in order to distinguish them from the solutions previously discussed which are labeled "rise." Although no large discrepancies exist during the early stage of the impact, appreciable differences between the calculated results are apparent after immersion of the sister keelson. For other conditions, even greater differences may be encountered. At zero trim, for instance, because of the instantaneous expansion of the intersected width, the assumption of a flat water surface (no rise) leads to the calculation of infinite loads on the float.

In view of the fact that present information is not sufficient to permit the determination of the conditions and shapes for which the rise may be safely neglected, it would appear that the calculation of the section characteristics is desirable. Since it is usually of interest to calculate a number of impact conditions for a given float, the additional effort required to obtain the section characteristics should not be a serious drawback.

CONCLUSIONS

An analysis was made to determine the hydrodynamic impact loads experienced by scalloped-bottom seaplanes in smooth and rough water. Although the agreement of the calculated results with specific test data is encouraging, a quantitative assessment of the method must necessarily be restricted by the very limited experimental data available. From such information it appears that:

1. On the basis of the analysis, which assumes that the primary flow occurs in transverse planes and that the virtual mass in any flow plane is determined by the modified section characteristics, a fairly good representation of the load-time variation during immersion may be calculated for vertical impacts at zero trim, as well as for the more general case of impacts at positive trim along flight paths inclined to the keel and to the water surface.

2. The analysis may be applied to approximate impacts in rough water if the initial conditions are taken relative to the wave slope.

3. For conventional float configurations no serious discrepancies are introduced by neglecting the warped bow and considering the float to have constant cross section.

4. For the trim angles which are believed to be representative of the main forebody impact in flight landings the afterbody seems to have little effect on the loads.

LANGLEY MEMORIAL AERONAUTICAL LABORATORY,
NATIONAL ADVISORY COMMITTEE FOR AERONAUTICS,
LANGLEY FIELD, VA., *April 16, 1947.*

APPENDIX A

WORKING EQUATIONS FOR CALCULATING SECTION CHARACTERISTICS

The section characteristics, which determine the variation of the virtual mass with penetration into a given flow plane, may be calculated for any arbitrary float shape by means of the following equations:

First scallop:

$$[u(c)]_{inner}=a_1+a_2c+a_3c^2+a_4c^3+a_5c^4+\ \ldots \tag{A1}$$

and

$$\zeta\Big|_0^{\zeta_{sk}}=a_1c+a_2\frac{c^2}{2}+a_3\frac{c^3}{3}+a_4\frac{c^4}{4}+a_5\frac{c^5}{5}+\ \ldots \tag{A2}$$

The coefficients a_1, a_2, . . . are obtained by solution of the system of equations represented by

$$\begin{bmatrix} A_{11}A_{12}A_{13} & \ldots & A_{1n} \\ A_{21}A_{22}A_{23} & \ldots & A_{2n} \\ A_{31}A_{32}A_{33} & \ldots & A_{3n} \\ \cdots\cdots\cdots & & \cdots \\ A_{m1}A_{m2}A_{m3} & \ldots & A_{mn} \end{bmatrix} \begin{bmatrix} a_1 \\ a_2 \\ a_3 \\ \cdots \\ a_n \end{bmatrix} = \begin{bmatrix} \zeta(c_1) \\ \zeta(c_2) \\ \zeta(c_3) \\ \cdots \\ \zeta(c_m) \end{bmatrix} \tag{A3}$$

where

$$A_{i1}=\frac{\pi}{2}c_i$$

$$A_{i2}=c_i^2$$

$$A_{i3}=\frac{\pi}{4}c_i^3$$

$$A_{i4}=\frac{2}{3}c_i^4$$

$$A_{i5}=\frac{3\pi}{16}=c_i^5$$

and so forth; and where c_i, $\zeta(c_i)$ are the coordinates of points chosen on the contour of the inner scallop.

The preceding equations are also applicable to floats and hulls having no discontinuities between the keel and chine. Second scallop:

$$[u(c)]_{outer}=b_1+b_2c+b_3c^2+b_4c^3+b_5c^4+\ \ldots \tag{A4}$$

and

$$\zeta\Big|_{\zeta_{sk}}^{\zeta_{ch}}=\zeta_{sk}+b_1(c-c_{sk})+\frac{b_2}{2}(c^2-c_{sk}^2)+\frac{b_3}{3}(c^3-c_{sk}^3)+$$

$$\frac{b_4}{4}(c^4-c_{sk}^4)+\frac{b_5}{5}(c^5-c_{sk}^5)+\ \ldots \tag{A5}$$

where

$$\zeta_{sk}=a_1c_{sk}+a_2\frac{c_{sk}^2}{2}+a_3\frac{c_{sk}^3}{3}+a_4\frac{c_{sk}^4}{4}+a_5\frac{c_{sk}^5}{5}+\ \cdots$$

The coefficients b_1, b_2, . . . are obtained by the solution of the system of equations represented by

$$\begin{bmatrix} B_{11}B_{12}B_{13} & \ldots & B_{1n} \\ B_{21}B_{22}B_{23} & \ldots & B_{2n} \\ B_{31}B_{32}B_{33} & \ldots & B_{3n} \\ \cdots\cdots\cdots & & \cdots \\ B_{m1}B_{m2}B_{m3} & \ldots & B_{mn} \end{bmatrix} \begin{bmatrix} b_1 \\ b_2 \\ b_3 \\ \cdots \\ b_n \end{bmatrix} = \begin{Bmatrix} [\Delta\zeta(c)]_1 \\ [\Delta\zeta(c)]_2 \\ [\Delta\zeta(c)]_3 \\ \cdots\cdots \\ [\Delta\zeta(c)]_m \end{Bmatrix} \tag{A6}$$

where

$$B_{i1}=c_i\Big(\frac{\pi}{2}-\sin^{-1}\frac{c_{sk}}{c_i}\Big)$$

$$B_{i2}=c_i\sqrt{c_i^2-c_{sk}^2}$$

$$B_{i3}=c_i\Big[\frac{c_i^2}{2}\Big(\frac{\pi}{2}-\sin^{-1}\frac{c_{sk}}{c_i}\Big)+\frac{c_{sk}}{2}\sqrt{c_i^2-c_{sk}^2}\Big]$$

$$B_{i4}=c_i\Big[c_i^2\sqrt{c_i^2-c_{sk}^2}-\frac{(c_i^2-c_{sk}^2)^{3/2}}{3}\Big]$$

$$B_{i5}=\frac{c_i}{4}\Big[c_{sk}\sqrt{c_i^2-c_{sk}^2}\Big(c_{sk}^2+\frac{3c_i^2}{2}\Big)+\frac{3c_i^4}{2}\Big(\frac{\pi}{2}-\sin^{-1}\frac{c_{sk}}{c_i}\Big)\Big]$$

and so forth, and

$$[\Delta\zeta(c)]_i=\zeta(c_i)-\zeta(c_i,t_{sk})$$

and

$$\zeta(c_i,t_{sk})=a_1c_i\sin^{-1}\frac{c_{sk}}{c_i}-a_2c_i(\sqrt{c_i^2-c_{sk}^2}-c_i)+$$

$$a_3c_i\Big[\frac{c_i^2}{2}\sin^{-1}\frac{c_{sk}}{c_i}-\frac{c_{sk}}{2}\sqrt{c_i^2-c_{sk}^2}\Big]+$$

$$a_4c_i\Big[\frac{(c_i^2-c_{sk}^2)^{3/2}}{3}-c_i^2\sqrt{c_i^2-c_{sk}^2}+\frac{2}{3}c_i^3\Big]-$$

$$\frac{a_5c_i}{4}\Big[c_{sk}\sqrt{c_i^2-c_{sk}^2}\Big(c_{sk}^2+\frac{3c_i^2}{2}\Big)+$$

$$\frac{3c_i^4}{2}\sin^{-1}\frac{c_{sk}}{c_i}\Big]+\cdots$$

and c_i, $\zeta(c_i)$ are the coordinates of points chosen on the contour of the outer scallop.

The same method may be applied to obtain similar equations for floats with any number of scallops or discontinuities by determining the shape of the free surface at the instant of initial penetration of the scallop in question from the coefficients for the scallop immediately preceding.

The section characteristics calculated by application of the preceding equations may be modified in accordance with the relation

$$\zeta_{mod}=\frac{\frac{\pi}{2}\cot\beta}{\frac{\pi}{2\beta}-1}\zeta_{calc} \tag{A7}$$

as previously discussed. The factor $\sqrt{0.82}$, which has been omitted from the modification, is included as part of one of the constants in the equations of motion (appendix B).

APPENDIX B

WORKING EQUATIONS OF MOTION AND SOLUTION OF TIME HISTORY

Before particular solutions are undertaken to calculate the loads and motions experienced by a specific float for given impact conditions, the modified section characteristics must be determined by means of the equations presented in appendix A. The section characteristics are properties of the float and may therefore be applied to the calculation of time-history solutions for as many impact conditions as may be desired.

On the basis of the flat-plate analogy

$$m_w = 0.82 \frac{\rho\pi}{2} [c(\zeta)]^2_{mod} \tag{B1}$$

where $[c(\zeta)]_{mod}$ is determined from the calculated section characteristics as modified in accordance with equation (A7). The factor 0.82 is the empirical correction determined by reference 1 which has been omitted from the modification and is included instead as a constant in the equations of motion.

Differentiating equation (B1)

$$\frac{dm_w}{d\zeta} = 0.82\rho\pi[c(\zeta)]_{mod} \frac{d}{d\zeta} [c(\zeta)]_{mod} = \frac{0.82\rho\pi[c(\zeta)]_{mod}}{[u(c)]_{mod}} \tag{B2}$$

In the equations which follow, $[c(\zeta)]_{mod}$ and $[u(c)]_{mod}$ will be referred to as c and u, respectively.

IMPACT NORMAL TO THE WATER AT ZERO TRIM

At zero trim the wetted area of the float in the plane of the water surface is rectangular; therefore,

$$A = \frac{l}{2c}$$

and

$$\frac{dA}{d\zeta} = -\frac{l \frac{dc}{d\zeta}}{2c^2} = -\frac{l}{2uc^2}$$

Equations of motion.—If the foregoing expressions for the virtual mass and the aspect ratio are incorporated, the equations of motion (1) and (2) for an impact normal to the water at zero trim may be written as

$$\dot{\zeta} = \frac{\dot{\zeta}_0}{1 + \frac{K_2}{M}(l-c)c^2} \tag{B3}$$

and

$$-\ddot{\zeta} = \frac{K_2\dot{\zeta}_0\dot{\zeta}(2l-3c)c}{Mu\left[1 + \frac{K_2}{M}(l-c)c^2\right]^2} \tag{B4}$$

where

$$K_2 = 0.82 \frac{\rho\pi}{2}$$

Time-history solution.—After the modified section characteristics have been calculated for the float under consideration by means of the equations of appendix A, specific time-history solutions of the variables may be obtained without recourse to step-by-step methods by the following procedure:

(1) Calculate the constants from the initial conditions.

(2) Substitute successive arbitrary value of the velocity $\dot{\zeta} \leqq \dot{\zeta}_0$ into equation (B3) to calculate the corresponding values of c. For any value of c the magnitudes of ζ and u are fixed by the section characteristics.

(3) With the values of the variables calculated in step 2 solve equation (B4) for $\ddot{\zeta}$.

(4) Calculate a sufficient number of simultaneous values of displacement, velocity, and acceleration to define the motion during the impact. (After some experience has been attained in selecting the velocities, only a relatively small number of points need be computed for each solution.)

(5) Integrate the variation of $1/\dot{\zeta}$ with ζ to obtain the time after contact at which each combination of the variables occurs.

OBLIQUE IMPACT AT POSITIVE TRIM

Equations of motion.—For the more general problem of a step impact at positive trim along an oblique flight path, incorporation of the foregoing expression for the virtual mass into equations (15) and (16) leads to the following equations of motion:

$$-\ddot{z} = \frac{c_s^2(\dot{z} + K_1 \cos \tau)^2}{\cos \tau \left(K_3 + \int_0^{\zeta_s} c_s^2 d\zeta_s\right)} \tag{B5}$$

and

$$K_3\left[\left(\frac{V_{v_0} + K_1 \cos \tau}{\dot{z} + K_1 \cos \tau}\right)e^\mu - 1\right] = \int_0^{\zeta_s} c_s^2 d\zeta_s \tag{B6}$$

where

$$K = \frac{1}{\tan \tau}\left(1 - \frac{\tan \tau}{2 \tan \beta}\right)$$

$$K_1 = (V_{h_0} - V_{v_0} \tan \tau) \sin \tau$$

$$K_2 = 0.82 \frac{\rho\pi}{2}$$

$$K_3 = \frac{W}{g}\left(\frac{1}{KK_2}\right)$$

and

$$\mu = K_1 \cos \tau \left[\frac{1}{V_{v_0} + K_1 \cos \tau} - \frac{1}{\dot{z} + K_1 \cos \tau}\right]$$

After chine immersion has occurred,

$$c_s = c_{s_{ch}} \qquad (B7)$$

and

$$\int_0^{\zeta_s} c_s{}^2 d\zeta_s = \int_0^{\zeta_{s_{ch}}} c_s{}^2 d\zeta_s + c_{s_{ch}}{}^2(\zeta_s - \zeta_{s_{ch}}) \qquad (B8)$$

Time-history solution—For the general case of impacts at positive trim, it is not necessary to compute u since the only section characteristics required are the variation of c_s with ζ_s and a plot of $\int_0^{\zeta_s} c_s{}^2 d\zeta_s$ against c_s. (See fig. 7). After the section characteristics have been calculated for a particular float, time-history solutions may be obtained for as many impact conditions as may be desired by a procedure similar to that previously discussed:

(1) Calculate the constants from the initial conditions.

(2) Substitute successive arbitrary values of the velocity $\dot{z} \leqq V_{v_0}$ into equation (B6), solve for the value of $\int_0^{\zeta_s} c_s{}^2 d\zeta_s$, and obtain the corresponding magnitudes of c_s and ζ_s from the curves. A calculated value of the integral greater than $\int_0^{\zeta_{s_{ch}}} c_s{}^2 d\zeta_s$ indicates that the velocity substituted corresponds to a time after chine immersion has occurred and requires the substitution of (B7) and (B8) in equation (B6). After

chine immersion $\int_0^{\zeta_{s_{ch}}} c_s{}^2 d\zeta_s$ is a constant and ζ_s may be calculated directly from equation (B6).

(3) Calculate $z = \zeta_s \cos \tau$.

(4) With the variables calculated above, solve equation (B5) for $\ddot{z}$.

(5) After a sufficient number of simultaneous values of displacement, velocity, and acceleration to define the motion during the impact have been calculated, integrate the variation of $1/\dot{z}$ with z to obtain the time after contact at which each combination of the variables occurs.

REFERENCES

1. Mayo, Wilbur L.: Analysis and Modification of Theory for Impact of Seaplanes on Water. NACA Rep. No. 810, 1945.
2. Mayo, Wilbur L.: Theoretical and Experimental Dynamic Loads for a Prismatic Float Having an Angle of Dead Rise of 22½°. NACA RB No. L5F15, 1945.
3. Pabst, Wilhelm: Theory of the Landing Impact of Seaplanes. NACA TM No. 580, 1930.
4. Wagner, Herbert: Über Stoss- und Gleitvorgänge an der Oberfläche von Flüssigkeiten. Z.f.a.M.M., Bd. 12, Heft 4, Aug. 1932, pp. 193–215.
5. Wagner, Herbert: Landing of Seaplanes. NACA TM No. 622, 1931.
6. Batterson, Sidney A.: The NACA Impact Basin and Water Landing Tests of a Float Model at Various Velocities and Weights. NACA Rep. No. 795, 1944.